nature genetics

Deficiency or inhibition of oxygen sensor Phd1 induces hypoxia tolerance by reprogramming basal metabolism

Julián Aragonés[1,2,20], Martin Schneider[1,2,19,20], Katie Van Geyte[1,2,20], Peter Fraisl[1,2,20], Tom Dresselaers[3], Massimiliano Mazzone[1,2], Ruud Dirkx[4], Serena Zacchigna[1,2], Hélène Lemieux[5], Nam Ho Jeoung[6], Diether Lambrechts[1,2], Tammie Bishop[7], Peggy Lafuste[1,2], Antonio Diez-Juan[1,2], Sarah K Harten[8], Pieter Van Noten[9], Katrien De Bock[9], Carsten Willam[7,19], Marc Tjwa[1,2], Alexandra Grosfeld[7], Rachel Navet[10], Lieve Moons[1,2], Thierry Vandendriessche[1,2], Christophe Deroose[11], Bhathiya Wijeyekoon[7], Johan Nuyts[11], Benedicte Jordan[12], Robert Silasi-Mansat[13], Florea Lupu[13], Mieke Dewerchin[1,2], Chris Pugh[7], Phil Salmon[14], Luc Mortelmans[11], Bernard Gallez[12], Frans Gorus[15], Johan Buyse[16], Francis Sluse[10], Robert A Harris[6], Erich Gnaiger[5], Peter Hespel[9], Paul Van Hecke[3], Frans Schuit[17], Paul Van Veldhoven[18], Peter Ratcliffe[7], Myriam Baes[4], Patrick Maxwell[8] & Peter Carmeliet[1,2]

HIF prolyl hydroxylases (PHD1–3) are oxygen sensors that regulate the stability of the hypoxia-inducible factors (HIFs) in an oxygen-dependent manner. Here, we show that loss of Phd1 lowers oxygen consumption in skeletal muscle by reprogramming glucose metabolism from oxidative to more anaerobic ATP production through activation of a Pparα pathway. This metabolic adaptation to oxygen conservation impairs oxidative muscle performance in healthy conditions, but it provides acute protection of myofibers against lethal ischemia. Hypoxia tolerance is not due to HIF-dependent angiogenesis, erythropoiesis or vasodilation, but rather to reduced generation of oxidative stress, which allows Phd1-deficient myofibers to preserve mitochondrial respiration. Hypoxia tolerance relies primarily on Hif-2α and was not observed in heterozygous Phd2-deficient or homozygous Phd3-deficient mice. Of medical importance, conditional knockdown of Phd1 also rapidly induces hypoxia tolerance. These findings delineate a new role of Phd1 in hypoxia tolerance and offer new treatment perspectives for disorders characterized by oxidative stress.

Oxygen is among the elements whose reduction provides the largest free energy release per electron transfer. Most multicellular organisms consume oxygen to meet metabolic needs, relying heavily on aerobic metabolism. Nonetheless, several species, such as birds living at high altitudes, fossorial mammals and diving animals, show hypoxia tolerance that enables them to survive in conditions of limiting oxygen supply[1]. Other species, such as hibernating mammals, estivating reptiles and dormant *Caenorhabditis elegans* dauer larvae, have developed mechanisms to conserve oxygen[1].

Central to hypoxia tolerance or oxygen conservation is a hypometabolic state characterized by a reduction in oxygen consumption, often more than tenfold[2]. Surprisingly little is known, however, about the molecular mechanisms underlying these adaptations. Oxygen conservation relies on a rapid, reversible metabolic switch from carbohydrate

[1]The Center for Transgene Technology and Gene Therapy, Katholieke Universiteit (K.U.) Leuven, Leuven, B-3000, Belgium. [2]Department of Transgene Technology and Gene Therapy, Flanders Institute for Biotechnology (VIB), Leuven, B-3000, Belgium. [3]Biomedical MRI Unit, K.U. Leuven, Leuven, B-3000, Belgium. [4]Laboratory of Cell Metabolism, K.U. Leuven, Leuven, B-3000, Belgium. [5]Medical University of Innsbruck, Department of Transplant Surgery, D. Swarovski Research Laboratory, Innsbruck, A-6020 Austria. [6]Department of Biochemistry and Molecular Biology, Indiana University School of Medicine, Indianapolis, Indiana 46202, USA. [7]The Henry Wellcome Building for Molecular Physiology, Oxford, OX3 7BN, UK. [8]Division of Medicine, Hammersmith Campus, Imperial College London, London, W12 ONN, UK. [9]Exercise and Health Laboratory, Faculty of Kinesiology and Rehabilitation Sciences, K.U. Leuven, B-3001 Leuven, Belgium. [10]Laboratory of Bioenergetics and Molecular Physiology, Department of Life Sciences, University of Liege, 4000 Liege, Belgium. [11]Department of Nuclear Medicine, University Hospital, K.U. Leuven, Leuven, B-3000 Belgium. [12]Biomedical Magnetic Resonance Unit, Medicinal Chemistry and Radiopharmacy, U.C. Louvain, B-1200 Brussels, Belgium. [13]Cardiovascular Research Program, Oklahoma Medical Research Foundation, Oklahoma 73104, USA. [14]Skyscan NV, B-2630 Aartselaar, Belgium. [15]Diabetes Research Center, Free University of Brussels, B-1090 Brussels, Belgium. [16]Laboratory for Physiology, Immunology and Genetics of Domestic Animals, Department of Biosystems, K.U. Leuven, Leuven, B-3001, Belgium. [17]Gene Expression Unit, Department of Molecular Cell Biology, K.U. Leuven, Leuven, B-3000, Belgium. [18]Department of Molecular Cell Biology, Laboratorium for Lipid Biochemistry and Protein Interactions (LIPIT), K.U. Leuven, B-3000 Belgium. [19]Current addresses: Department of General, Visceral and Transplantation Surgery, University of Heidelberg, D-69120 Heidelberg, Germany (M.S.) and Department of Nephrology and Hypertension, University of Erlangen-Nuremberg, D-91054 Erlangen, Germany (C.W.). [20]These authors contributed equally to this work. Correspondence should be addressed to P.C. (peter.carmeliet@med.kuleuven.be).

Received 30 July 2007; accepted 23 October 2007; published online 6 January 2008; doi:10.1038/ng.2007.62

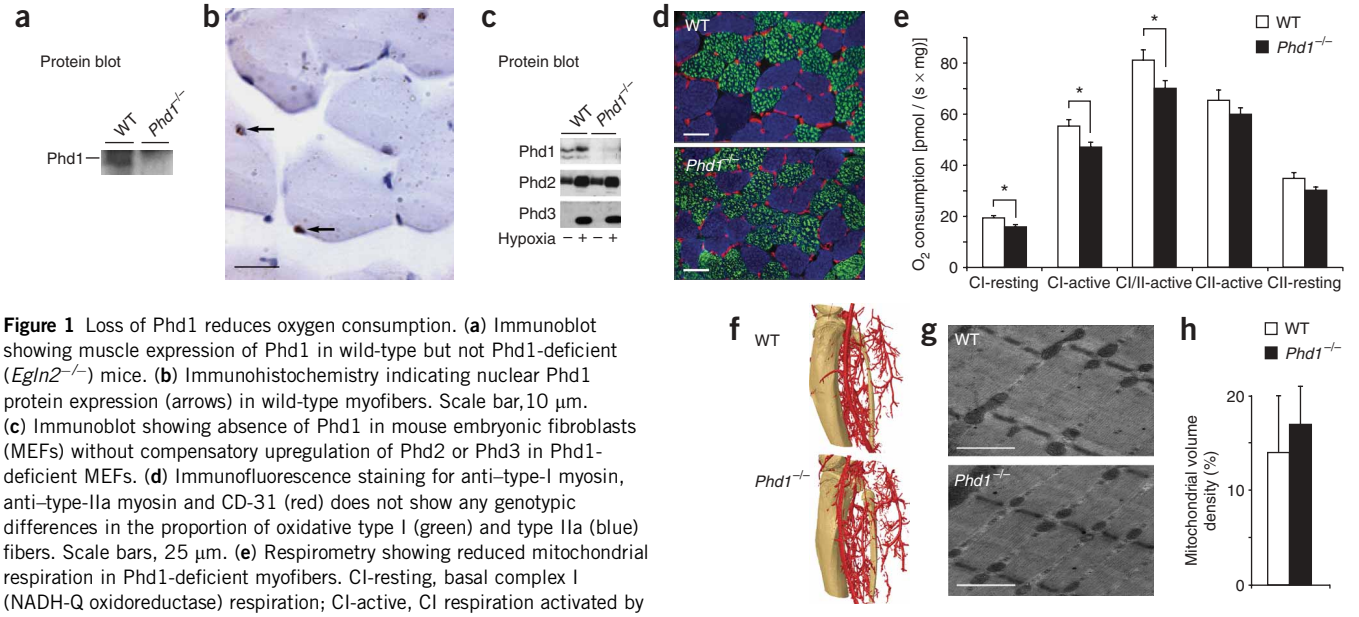

Figure 1 Loss of Phd1 reduces oxygen consumption. (**a**) Immunoblot showing muscle expression of Phd1 in wild-type but not Phd1-deficient (*Egln2*$^{-/-}$) mice. (**b**) Immunohistochemistry indicating nuclear Phd1 protein expression (arrows) in wild-type myofibers. Scale bar,10 μm. (**c**) Immunoblot showing absence of Phd1 in mouse embryonic fibroblasts (MEFs) without compensatory upregulation of Phd2 or Phd3 in Phd1-deficient MEFs. (**d**) Immunofluorescence staining for anti–type-I myosin, anti–type-IIa myosin and CD-31 (red) does not show any genotypic differences in the proportion of oxidative type I (green) and type IIa (blue) fibers. Scale bars, 25 μm. (**e**) Respirometry showing reduced mitochondrial respiration in Phd1-deficient myofibers. CI-resting, basal complex I (NADH-Q oxidoreductase) respiration; CI-active, CI respiration activated by excess of ADP; CI/II-active, combined CI and CII (complex II, succinate dehydrogenase) respiration; CII-active, CII respiration after inhibition of CI; CII-resting, CII respiration after inhibition of ATP/ADP translocase. Mean ± s.e.m. of 22–33 myofiber preparations from five mice per genotype. * $P < 0.05$. (**f**) Micro-CT angiograms of lower hindlimbs in baseline conditions showing comparable morphology and numbers of smaller arterial and arteriolar branches. (**g**) Transmission electron micrographs of soleus muscle indicating similar ultrastructure and cristae content of mitochondria in baseline wild-type and Phd1-deficient mice. Scale bars, 0.5 μm. (**h**) Comparable mitochondrial volume density in wild-type and Phd1-deficient skeletal muscle. Mean ± s.e.m., $n = 3$. WT, wild type.

oxidation to anaerobic glycolysis[3,4] through upregulation of pyruvate dehydrogenase kinases (PDKs) that restrict the entry of glycolytic intermediates into the tricarboxylic acid (TCA) cycle[5]. Hypoxia-inducible transcription factors (HIFs) have also been implicated in regulating these metabolic adaptations[3,4].

Aerobic organisms are equipped with mechanisms to sense changes in oxygen tension. The HIF prolyl hydroxylases (PHD1–3) are oxygen-sensitive enzymes that regulate the stability of HIFs and thereby induce cellular adaptations in response to hypoxia[6,7]. Knockdown of PHDs enhances HIF-dependent gene expression *in vitro*[8,9], whereas inhibition of prolyl hydroxylation increases vessel growth[10,11]. A recent study reported a role of Phd2 (encoded by *Egln1*) in placentation, but the roles of Phd1 (encoded by *Egln2*) and Phd3 (encoded by *Egln3*) remain enigmatic[12]. It also remains largely unknown whether and to what extent PHDs have overlapping or unique tissue-specific activities in disease, or which molecules are downstream targets of PHDs (in particular, whether HIFs are the only targets).

Oxygen consumption has been linked to the formation of reactive oxygen species (ROS), especially in hypoxic conditions[3,4], and oxygen conservation has been suggested to improve the survival response to severe acute hypoxia in highlanders[13]. We therefore characterized the role of Phd1 in oxygen consumption and hypoxia tolerance. Because of its large mass and important contribution to total body oxygen consumption, skeletal muscle has a central role in metabolism[14]. Here, we show that loss of Phd1 lowers oxygen consumption by reprogramming basal metabolism. This pathway relies, in part, on the activation of the metabolic master switch Pparα which, via upregulation of its downstream target Pdk4, restricts entry of glycolytic intermediates into the TCA cycle. Although impairing oxidative muscle performance in healthy conditions, the enhanced oxygen conservation protects Phd1-deficient myofibers against severe acute ischemia by preventing excess oxidative damage.

RESULTS

Generation of mice lacking Phd1

We first analyzed the expression of Phd1 in skeletal muscle. Phd1 was detectable in skeletal muscle at the mRNA (data not shown) and protein levels (**Fig. 1a**). Immunostaining confirmed that myofibers express Phd1 (**Fig. 1b**). To study the role of Phd1 in skeletal muscle, we generated Phd1-deficient (*Egln2*$^{-/-}$) mice, which were healthy (**Supplementary Note** and **Supplementary Fig. 1** online). Loss of Phd1 did not cause any compensatory upregulation of Phd2 or Phd3 (**Fig. 1c**), nor did it cause a switch in myofiber type (**Fig. 1d**).

Reduced oxygen consumption by Phd1$^{-/-}$ skeletal myofibers

Indirect calorimetry showed that whole body oxygen consumption was reduced in Phd1-deficient mice (oxygen consumption, ml per hour per gram body weight: 4.0 ± 0.04 in wild-type versus 3.5 ± 0.04 in Phd1-deficient mice; $n = 7$, $P < 0.0005$). We detected similar oxygen conservation during the day, when mice are inactive (data not shown). As skeletal muscle constitutes 40–50% of the body mass and is responsible for 40–50% of the oxygen consumption in resting conditions[15], oxygen consumption by Phd1-deficient muscle was likely reduced. We therefore used high-resolution respirometry of permeabilized muscle to measure mitochondrial respiration through complex I (by supplementing pyruvate + malate) or complex II (by including succinate). When electron transport through both complexes was activated and excess ADP was added, respiration was reduced in Phd1-deficient myofibers (**Fig. 1e**). This defect was specific for complex I, as respiration through complex II did not show a significant reduction (**Fig. 1e**). Similar findings were obtained when we included octanoyl carnitine (data not shown). Taken together, these data indicated that respiration in Phd1-deficient myofibers was reduced.

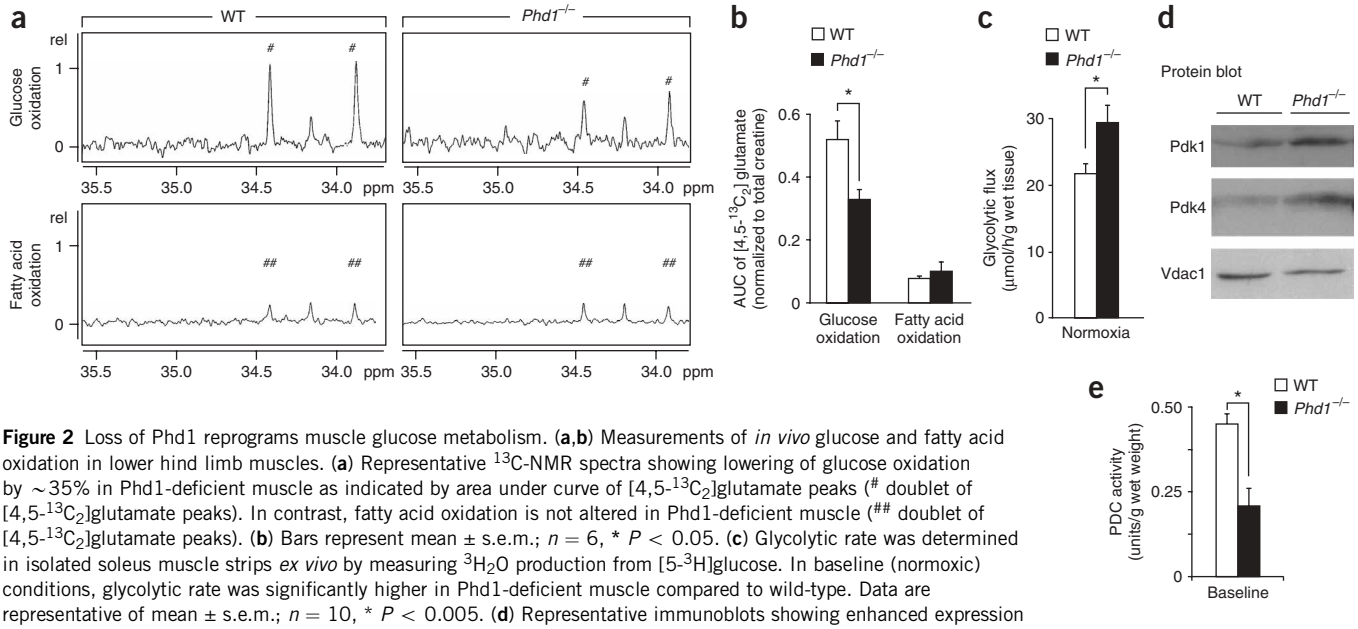

Figure 2 Loss of Phd1 reprograms muscle glucose metabolism. (**a**,**b**) Measurements of *in vivo* glucose and fatty acid oxidation in lower hind limb muscles. (**a**) Representative ^{13}C-NMR spectra showing lowering of glucose oxidation by ~35% in Phd1-deficient muscle as indicated by area under curve of [4,5-$^{13}C_2$]glutamate peaks (# doublet of [4,5-$^{13}C_2$]glutamate peaks). In contrast, fatty acid oxidation is not altered in Phd1-deficient muscle (## doublet of [4,5-$^{13}C_2$]glutamate peaks). (**b**) Bars represent mean ± s.e.m.; $n = 6$, * $P < 0.05$. (**c**) Glycolytic rate was determined in isolated soleus muscle strips *ex vivo* by measuring ^3H_2O production from [5-^{3}H]glucose. In baseline (normoxic) conditions, glycolytic rate was significantly higher in Phd1-deficient muscle compared to wild-type. Data are representative of mean ± s.e.m.; $n = 10$, * $P < 0.005$. (**d**) Representative immunoblots showing enhanced expression of Pdk1 and Pdk4 protein in baseline muscle lysates from Phd1-deficient mice. Voltage-dependent anion channel (Vdac1) was used to assure equal loading. (**e**) Measurements of the actual (as extracted from baseline muscle tissue, without activation by dephosphorylation) activity of the PDC, indicating significantly decreased PDC activity in Phd1-deficient mice. Data are representative of mean ± s.e.m.; $n = 3$, * $P = 0.015$. WT, wild type.

The reduced oxygen consumption was not attributable to genotypic differences in mitochondrial biogenesis, oxygen delivery, erythropoiesis or vascularization (**Fig. 1f–h** and **Supplementary Note**) or to perfusion of crural muscles (ml/g/min: 0.39 ± 0.02 in wild-type versus 0.35 ± 0.03 in Phd1-deficient mice; $n = 4$, P = n.s.). As a result of the oxygen conservation, oxidative muscle performance was impaired in Phd1-deficient mice. Indeed, when Phd1-deficient mice were forced to run uphill in a treadmill, an exercise that recruits primarily oxidative crural muscle fibers and relies on oxidative metabolism[16,17], they showed worse exercise endurance than wild-type mice (running time: 53.7 ± 1.8 min for wild-type versus 44.7 ± 3.6 min for Phd1-deficient mice; $n = 16$; $P = 0.03$).

Shift to anaerobic glucose utilization in Phd1$^{-/-}$ muscle

To study the metabolic mechanisms by which loss of Phd1 conserved oxygen, we analyzed glucose and fatty acid homeostasis. *In vivo* ^{13}C-NMR measurements of [^{13}C]glutamate resonances in muscle extracts after infusion of [U-$^{13}C_6$]glucose indicated that glucose oxidation was ~35% lower in Phd1-deficient mice. Indeed, [4,5-$^{13}C_2$]glutamate, expressed as a ratio versus total creatine, was significantly reduced in Phd1-deficient muscle (**Fig. 2a**,**b**). *Ex vivo* analysis using isolated muscles confirmed that oxidation of [U-^{14}C]glucose, measured by the production of $^{14}CO_2$ (ref. 18), was also reduced in Phd1-deficient mice (nmol glucose/h/g wet tissue: 1,190 ± 50 in wild-type versus 990 ± 56 in Phd1-deficient mice; $n = 12$; $P = 0.04$). However, loss of Phd1 did not completely shut down glucose oxidation, as occurs in fasting or hibernation[2,19]. This effect was specific, as ^{13}C-NMR measurements of [^{13}C]glutamate resonances in muscle extracts after whole animal infusion of [U-^{13}C]fatty acids showed that fatty acid oxidation was not altered in Phd1-deficient mice (**Fig. 2a**,**b**).

Glycolytic flux, measured by ^3H_2O production from [5-^{3}H]glucose in isolated soleus muscle, was increased in Phd1-deficient muscle in normoxic conditions (**Fig. 2c**). Metabolic profiling of muscle metabolic intermediates of the glycolytic pathway also showed an increase in 2-phosphoglycerate (**Table 1**). However, this increase in glycolysis was not due to an increase in blood glucose or insulin concentrations (**Table 1**), expression of glycolytic enzymes (**Table 2**) or glycogen content (data not shown) in the muscle.

Loss of Phd1 reduces entry of pyruvate into the TCA cycle

The reduced glucose oxidation and oxygen consumption raised the question of whether entry of glycolytic intermediates into the TCA cycle was reduced in the absence of Phd1. We therefore analyzed the

Table 1 Metabolites in baseline wild-type (WT) and Phd1-deficient (*Egln2*$^{-/-}$) muscle

		WT	*Egln2*$^{-/-}$
Plasma or serum	Glucose (mg/dl)	128 ± 5	122 ± 5
	Free fatty acid (mM)	0.19 ± 0.03	0.16 ± 0.03
	Insulin (ng/ml)	0.12 ± 0.05	0.09 ± 0.02
Muscle	Glucose 6-phosphate + fructose 6-phosphate	1.3 ± 0.1	1.8 ± 0.6
	Fructose 1,6-bisphosphate	0.03 ± 0.002	0.05 ± 0.01
	Glyceraldehyde 3-phosphate	0.01 ± 0.003	0.01 ± 0.001
	Dihydroxyacetone phosphate	0.05 ± 0.004	0.06 ± 0.01
	2-Phosphoglycerate	0.007 ± 0.001	0.013 ± 0.001*
	Phosphoenolpyruvate	0.02 ± 0.002	0.03 ± 0.001
	Triglycerides	6.1 ± 0.7	6.4 ± 0.4
	Phospholipids	18.3 ± 0.3	17.9 ± 0.6

Data are presented as mean ± s.e.m. ($n = 3$). *$P < 0.01$. Concentrations of all muscle metabolites are expressed as μM.

Table 2 Relative gene expression in Phd1-deficient (*Egln2*$^{-/-}$) muscle

	Baseline	
	WT	*Egln2*$^{-/-}$
Peroxisome proliferator-activated receptor α (*Ppara*)	1.00 ± 0.07	2.01 ± 0.32**
Peroxisome proliferator-activated receptor δ (*Ppard*)	1.00 ± 0.09	1.21 ± 0.14
Pyruvate dehydrogenase kinase isoenzyme 1 (*Pdk1*)	1.00 ± 0.17	1.58 ± 0.42*
Pyruvate dehydrogenase kinase isoenzyme 2 (*Pdk2*)	1.00 ± 0.18	1.17 ± 0.17
Pyruvate dehydrogenase kinase isoenzyme 4 (*Pdk4*)	1.00 ± 0.08	1.85 ± 0.21**
Hexokinase 4 (*Gck*)	1.00 ± 0.36	1.28 ± 0.19
Phosphofructokinase-M (*Pfkm*)	1.00 ± 0.12	0.87 ± 0.11
Glyceraldehyde 3-phosphate dehydrogenase (*Gapdh*)	1.00 ± 0.12	0.95 ± 0.10
Phosphoglycerate kinase (*Pgk1*)	1.00 ± 0.12	1.02 ± 0.13
Pyruvate kinase, muscle (*Pkm2*)	1.00 ± 0.07	1.19 ± 0.06

Quantitative RT-PCR data are presented as mean ± s.e.m. (n = 10–20), relative to the expression in baseline conditions in wild-type (WT) mice. *P < 0.05, **P < 0.01 versus baseline WT. No significant genotypic differences in the expression were observed for the following genes: *Ppard*, *Pdk2*, *Gck*, *Pfkm*, *Gapdh*, *Pgk1* and *Pkm2*.

expression of PDKs, which inhibit the activity of the pyruvate dehydrogenase complex (PDC) required for the conversion of pyruvate to acetyl CoA[20]. Concentrations of Pdk1 and Pdk4 RNAs and proteins were upregulated in Phd1-deficient muscle (**Table 2** and **Fig. 2d**). This regulation was specific, as *Pdk2* expression was not affected (**Table 2**). The increase in Pdk4 and Pdk1 concentrations was relevant, as PDC activity was reduced by 54% in Phd1-deficient muscles (**Fig. 2e**). However, this reduction was not as complete as that observed during fasting (93% reduction; data not shown) or hibernation[2,19].

Phd1$^{-/-}$ muscle is protected against ischemic necrosis

We next determined whether this reprogramming of basal metabolism and adaptation to oxygen conservation was relevant for the response to ischemia (**Fig. 3**). Mice were subjected to femoral artery ligation, which reduces perfusion by 70% and causes acute, severe ischemia. Histological analysis showed extensive ischemic damage in wild-type mice after 7 d of ischemia (**Fig. 3a**). Myofiber damage was more severe and occurred earlier in the soleus and plantaris muscles, indicating that oxidative myofibers were most sensitive. Compared to the total crural muscle area in unligated limbs (8.7 ± 0.7 mm^2), up to 83% was necrotic in ischemic wild-type muscles (7.2 ± 1.1 mm^2; n = 8), whereas, notably, ischemic Phd1-deficient muscles showed almost no necrosis (necrotic area of 0.8 ± 0.5 mm^2 in Phd1-deficient mice; n = 8; P < 0.001; **Fig. 3b**). The role of Phd1 was specific, as ischemic muscle was severely necrotic in heterozygous Phd2-deficient (*Egln1*$^{+/-}$) and homozygous Phd3-deficient (*Egln3*$^{-/-}$) mice (**Fig. 3c,d**). Heterozygous Phd1-deficient (*Egln2*$^{+/-}$) muscles were also not protected (necrotic area of 5.9 ± 1.4 mm^2; n = 8; P = n.s.).

Phd1-deficient myofibers are hypoxia tolerant

We explored whether the survival of ischemic Phd1-deficient muscles 7 d after femoral artery ligation was attributable to enhanced tissue regeneration. In contrast to wild-type muscle, muscle fibers in Phd1-deficient mice did not show any signs of regeneration or satellite cell activation or proliferation (**Fig. 3e–h**). We therefore suspected that Phd1-deficient myofibers were protected against ischemic necrosis. Indeed, extensive necrosis was detected in wild-type but not Phd1-deficient muscle after 48 h of ischemia (**Fig. 3i,j**). Immunolabeling of activated caspase-3 indicated that wild-type but not Phd1-deficient myofibers showed signs of apoptosis, most prominently in oxidative myofibers, within 4 h of ischemia (**Fig. 3m,n**). By electron microscopy, mitochondrial ultrastructure was also better preserved in ischemic Phd1-deficient myofibers (**Fig. 3o,p**; cristae surface density: 13.8 ± 1.7 μm^{-1} in wild-type versus 26.3 ± 4.2 μm^{-1} in Phd1-deficient mice; n = 3; P = 0.05). Loss of Phd1 rendered myofibers hypoxia tolerant in other models as well, including a transient hindlimb ischemia-reperfusion model that is known to cause extensive muscle damage through oxidative stress[21] (**Fig. 3k,l**). Thus, loss of Phd1 (*Egln2*$^{-/-}$), but not of Phd2 (*Egln1*$^{+/-}$) or Phd3 (*Egln3*$^{-/-}$), provided protection against ischemic muscle cell death. Obviously, the hypoxia tolerance was not absolute, as Phd1-deficient cells died when exposed to prolonged anoxia, such as that in 'no flow' models of organ ischemia (data not shown).

Hypoxic Phd1$^{-/-}$ myofibers consume less oxygen

We then analyzed whether various biological processes known to be regulated by HIFs, such as angiogenesis, vasodilation and erythropoiesis[22], underlay the hypoxia tolerance. However, hypoxia tolerance of Phd1-deficient myofibers was not attributable to the formation of supernumerary (collateral) vessels or to an accelerated revascularization of ischemic limbs, nor was it due to enhanced erythropoiesis, elevated myoglobin levels or an increased compensatory vasodilation after femoral artery ligation (**Supplementary Note**). Perfusion of ischemic hindlimbs was also comparable in both genotypes (muscle perfusion 2 h postligation, ml/g/min: 0.13 ± 0.04 in wild-type mice versus 0.15 ± 0.03 in Phd1-deficient mice; n = 4; P = n.s.).

Electron paramagnetic resonance (EPR) oximetry further showed that oxygen delivery was comparable in both genotypes in baseline and ischemic conditions (**Fig. 4a**). Because loss of Phd1 lowers myofiber oxygen consumption in baseline conditions, we scored intracellular oxygen levels by staining myofibers for pimonidazole, a marker of hypoxia. As myofibers started to die beyond 6 h of ischemia, we stained myofibers after 2 h of ischemia, when myofibers are still metabolically active. Ischemic wild-type myofibers stained strongly for pimonidazole, indicating intracellular hypoxia and thus suggesting that, despite a reduced supply of oxygen, they continued to consume oxygen (**Fig. 4b**)[23]. In contrast, ischemic Phd1-deficient muscles did not bind pimonidazole (**Fig. 4c**), indicating that Phd1-deficient myofibers consumed less oxygen. Thus, despite similar extracellular oxygen levels, intracellular oxygen levels differed markedly between the two genotypes.

Reduced oxidative stress in ischemic Phd1-deficient muscle

Oxygen consumption in conditions of low oxygen availability is associated with mitochondrial formation of reactive oxygen species (ROS)[3,24], and oxidative stress is a major cause of hypoxic skeletal muscle injury[21]. Because hypoxic tolerance has been associated with reduced oxidative stress[25], we analyzed whether hypoxic tolerance of Phd1-deficient myofibers was due to reduced generation of oxidative stress. First, the fraction of the antioxidant glutathione (GSH) that was oxidized to GS-SG was increased in ischemic wild-type but not

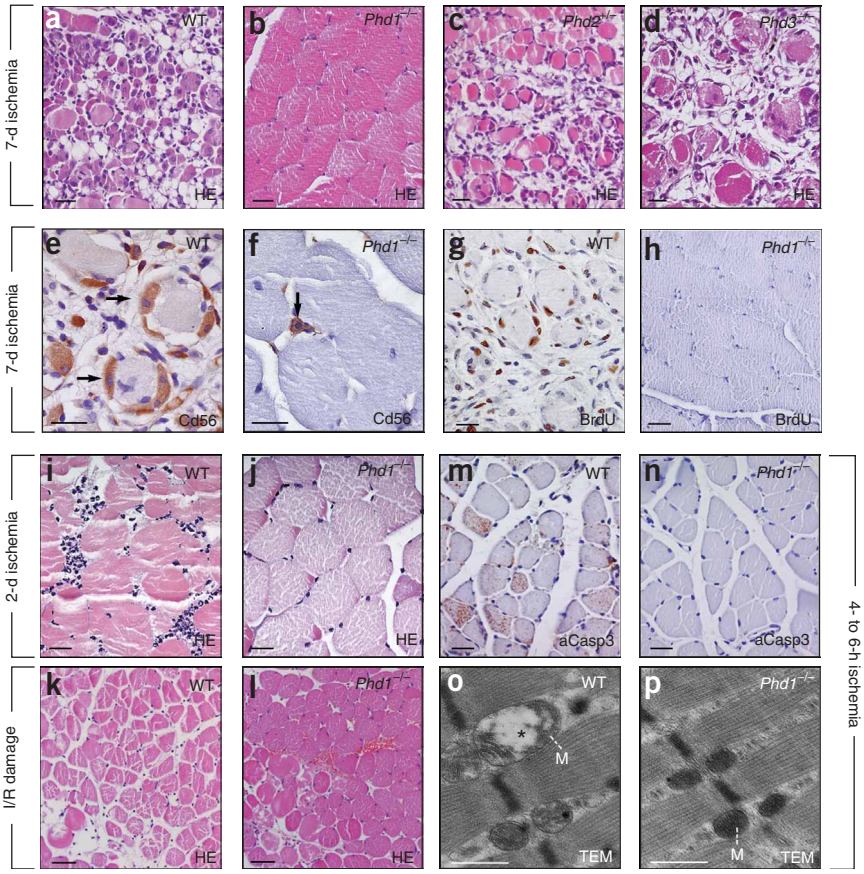

Figure 3 Hypoxia tolerance in ischemic Phd1-deficient muscle. (**a–h**) Representative histopathology of gastrocnemius muscle 7 d after induction of ischemia. Hematoxylin-eosin (HE) staining shows muscle necrosis, inflammation, fibrosis and myofiber regeneration in wild-type (**a**), heterozygous Phd2-deficient (*Egln1*$^{+/-}$; **c**) and homozygous Phd3-deficient (*Egln3*$^{-/-}$; **d**) mice (the generation of targeted Phd2 and Phd3 knockout mice will be reported elsewhere), but not in Phd1-deficient (*Egln2*$^{-/-}$) mice (**b**). Cd56-immunostaining indicates abundant myogenic precursor cells (arrows) in wild-type muscle (**e**), and quiescent Cd56^{+} satellite cells in ischemic Phd1-deficient muscle (arrow; **f**). BrdU-staining reveals multiple proliferating regenerating myofibers in wild-type (**g**) but not in Phd1-deficient muscle (**h**). (**i**,**j**) Histopathology of gastrocnemius muscle 2 d after induction of hindlimb ischemia. Hematoxylin-eosin staining shows extensive coagulation necrosis and inflammatory cell infiltrates in wild-type muscle (**i**) but entirely healthy myofibers in ischemic Phd1-deficient muscle (**j**). (**k**,**l**) Representative histopathology of the hindlimb musculature after ischemia-reperfusion (3–24 h), revealing extensive myofiber necrosis in wild-type mice (**k**), with only minimal myofiber damage in Phd1-deficient mice (**l**). (**m**,**n**) Soleus muscle 4 h after onset of ischemia. Immunostaining for activated caspase-3 shows apoptotic myofibers in wild-type (**m**) but not Phd1-deficient muscle (**n**). Scale bars in **a–j**,**m**,**n**, 25 μm; in **k**,**l**, 50 μm. (**o**,**p**) Transmission electron micrographs of soleus muscle after 6 h of ischemia showing swollen mitochondria (M) in wild-type muscle (**o**), with increased lucency of the inner compartment and fractured cristae (cristolysis, asterisk). In contrast, mitochondria in ischemic Phd1-deficient muscle are healthy and lack signs of ultrastructural damage (**p**). Scale bars in **o**,**p**, 0.5 μm. WT, wild-type.

Phd1-deficient muscle after 6 h of ischemia (percentage of baseline levels: 180 ± 19% in wild-type versus 111 ± 8% in Phd1-deficient mice; $n = 9$; $P = 0.005$). Second, after 3 h of ischemia, wild-type but not Phd1-deficient myofibers stained strongly for 8-hydroxy-2-deoxy guanosine (8-OHdG), a marker of deoxyguanosine oxidation[26], especially oxidative fibers (8-OHdG^{+} nuclei per optical field, fold increase versus baseline: 7.5 ± 1.7 in wild-type mice versus 3.3 ± 1.0 in Phd1-deficient mice; $n = 5$; $P = 0.05$; **Fig. 4d–g**). Third, after 6 h of ischemia, protein carbonylation was induced in ischemic wild-type but only minimally in ischemic Phd1-deficient muscle (densitometry, percentage of baseline: 390 ± 91% in wild-type versus 140 ± 39% in Phd1-deficient mice; $n = 5$; $P = 0.03$; **Fig. 4h**). Thus, loss of Phd1 reduced the formation of ROS in ischemic myofibers.

Reduced mitochondrial damage in ischemic Phd1$^{-/-}$ myofibers

ROS are well known to damage mitochondria and impair mitochondrial metabolism[27]. Consistent with reduced oxidative stress, mitochondrial performance was less severely impaired in ischemic Phd1-deficient myofibers. First, state 3 respiration of isolated muscle mitochondria (known to be sensitive to ischemic insults) was severely impaired in ischemic wild-type muscle, but not (or only minimally) in Phd1-deficient muscle (**Supplementary Note**). Furthermore, mitochondrial succinate dehydrogenase and aconitase, both of which contain iron-sulfur groups and are therefore sensitive to oxidation by ROS[28], remained more functional in ischemic Phd1-deficient myofibers (**Fig. 4i,j**). This effect was specific, as the activity of citrate synthase was not affected (U/mg protein, in baseline and ischemia: 0.12 ± 0.01 and 0.10 ± 0.01 in wild-type mice versus 0.11 ± 0.01 and 0.12 ± 0.005 in Phd1-deficient mice; $n = 7$; $P =$ n.s.). The functional preservation of ischemic Phd1-deficient mitochondria is consistent with their reduced structural damage (see above).

Phd1$^{-/-}$ myofibers produce ATP despite ischemia

^{31}P-NMR analysis of energy-rich phosphates in hindlimb muscles of live mice showed that, in acute ischemia, skeletal muscle ATP concentrations are initially maintained through rapid breakdown of phosphocreatine (PCr) by creatine kinase, an enzyme that transfers high-energy phosphates from PCr to ADP to generate ATP. In wild-type mice, PCr concentrations progressively declined over 120 min after onset of ischemia (**Fig. 4k,l**), whereas inorganic phosphate (P_i) concentrations steadily increased, indicating that the rate of ATP utilization exceeded the rate of oxidative and glycolytic ATP regeneration. In contrast, in Phd1-deficient mice, muscle PCr contents decreased only during the first 30 min after onset of ischemia, after which they stabilized and even tended to increase during prolonged ischemia (**Fig. 4l**). Thus, loss of Phd1 protected myofibers against complete ischemia-induced energy depletion.

Generation of energy in ischemic Phd1$^{-/-}$ myofibers

We then analyzed how Phd1-deficient myofibers were capable of generating ATP despite the severe reduction in oxygen supply. When infusing [U-$^{13}C_6$] glucose *in vivo* after 4 h of ischemia and measuring

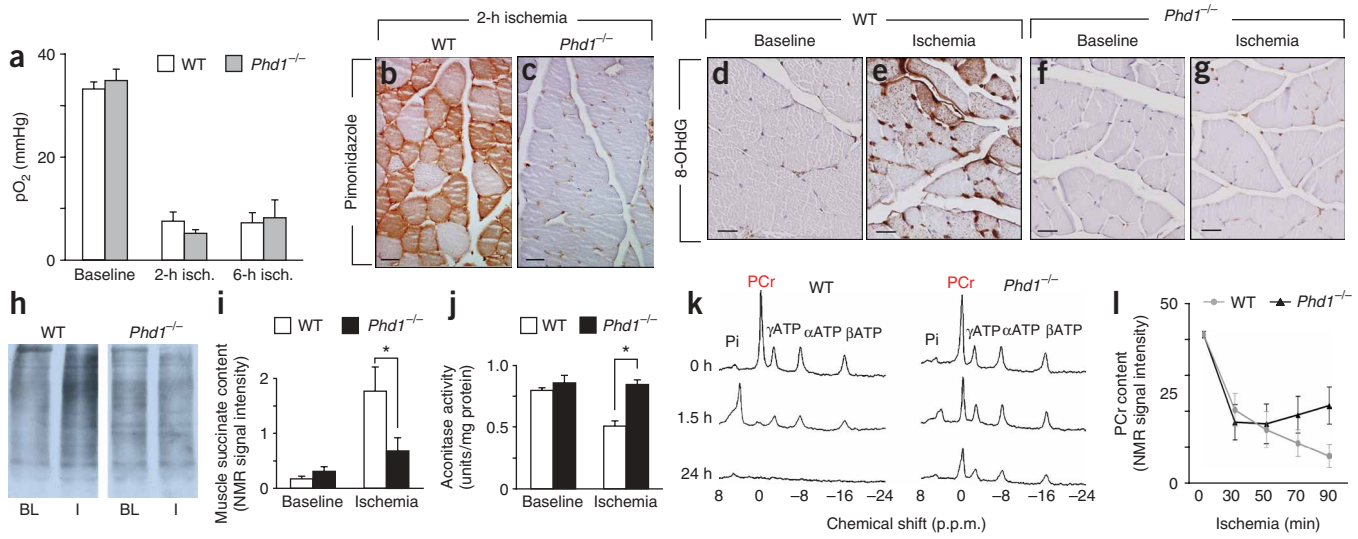

Figure 4 Reduced oxidative stress and energy production in ischemic Phd1-deficient muscle. (**a**) EPR oximetry showing comparable extracellular pO_2 in baseline and ischemic muscles of both genotypes (mean ± s.e.m.; $n = 4$). (**b**,**c**) Pimonidazole staining of soleus myofibers in ischemic (2 h) wild-type (**b**) but not Phd1-deficient mice (**c**). (**d–g**) Enhanced 8-Hydroxy-2-deoxyguanosine (8-OHdG) immunostaining of ischemic (3 h) wild-type (**e**) but not ischemic Phd1-deficient (**g**) muscle. (**h**) Immunoblots showing increased protein carbonylation in ischemic (I) wild-type but not in Phd1-deficient muscle. Equal amounts of protein were loaded in baseline (BL) and ischemic (I) conditions (6 h). (**i**) ^{1}H-NMR spectroscopy indicating accumulation of succinate in ischemic wild-type but not Phd1-deficient muscle (mean ± s.e.m. of values normalized to total creatine; * $P < 0.05$, $n = 6$). (**j**) Gastrocnemius aconitase enzyme activity is reduced after 6 h of ischemia in wild-type but not Phd1-deficient muscle (mean ± s.e.m.; * $P < 0.01$; $n = 3$). (**k**) Representative ^{31}P-NMR spectra showing comparable sources of energy-rich phosphates (PCr, γ, α, β-ATP) in wild-type and Phd1-deficient muscles in baseline conditions (0 h; that is, before ligation) and depletion of energy-rich phosphates and conversion to inorganic phosphate (P_i) in wild-type but not ischemic Phd1-deficient muscle at 1.5 and 24 h after ligation. (**l**) NMR spectroscopy showing progressive depletion of phosphocreatine (PCr) during the initial 30 min of ischemia in both genotypes, but subsequent recovery in ischemic Phd1-deficient muscle; mean ± s.e.m. of NMR signal intensity; $n = 3$. PCr data are expressed as percentage of the total phosphorus signal ($t = 0$ value based on non-ligated, contralateral limb). WT, wild type.

[^{13}C]glutamate resonances in ischemic muscle extracts by ^{13}C-NMR, we found that, as expected, glucose oxidation in ischemic muscles was reduced in both genotypes compared to baseline conditions. Notably, however, glucose oxidation was completely arrested in ischemic wild-type but not in Phd1-deficient myofibers ([4,5-$^{13}C_2$]glutamate peak, percentage of total creatine: 0.03 ± 0.02% in wild-type mice versus 0.18 ± 0.06% in Phd1-deficient muscle; $n = 6$; $P < 0.05$). In fact, compared to the corresponding baseline values, glucose oxidation in ischemic wild-type and Phd1-deficient myofibers proceeded at <5% and 50% of its normal rate, respectively. The complete elimination of glucose oxidation in ischemic wild-type myofibers results from the severe oxidative mitochondrial damage (see above). We observed similar findings when we analyzed fatty acid oxidation (**Supplementary Note**). Therefore, preserved mitochondria in ischemic Phd1-deficient myofibers are still competent to oxidize glucose and fatty acids, albeit at 50% of the normal rate in baseline conditions.

We also studied whether enhanced glycolytic flux contributed to the ability of Phd1-deficient myofibers to produce sufficient energy in low-oxygen conditions. Measurements in isolated muscles *ex vivo* showed that glycolytic flux was increased in Phd1-deficient fibers during 6 h of low-oxygen conditions (μmol glucose/h/g wet tissue: 29.3 ± 0.3 in wild-type versus 48.2 ± 0.5 in Phd1-deficient mice; $n = 10$; $P = 0.002$).

Role of Pparα in hypoxia tolerance induced by loss of Phd1

It is well established that the expression of Pdk4 is upregulated by the metabolic regulator Pparα[29]. Notably, loss of Phd1 upregulated the expression of Pparα (encoded by *Ppara*) in the muscle at the mRNA (**Table 2**) and protein levels (percentage of wild-type expression: 470 ± 40%; $n = 3$; $P = 0.001$). The induction of Pparα was specific, as expression of Pparδ, a key regulator of skeletal muscle mitochondrial biogenesis and fatty acid oxidation[14], was not affected by Phd1 deficiency (**Table 2**). Moreover, partial knockdown of Pparα in muscles of Phd1-deficient mice *in vivo* through electroporation of $shPpar\alpha^{KD}$ construct, reducing *Ppara* expression to 58 ± 6% relative to the control $shPpar\alpha^{CTR}$ construct ($n = 10$; $P = 0.012$), also lowered expression of *Pdk4* (78 ± 6% of $shPpar\alpha^{CTR}$, $n = 12$; $P = 0.03$). The $shPpar\alpha^{CTR}$ construct, used as a control, differed from $shPpar\alpha^{KD}$ by a mismatch of ten nucleotides in the sequence of *Ppara*.

To strengthen the link between Pdk4 and Pparα and to assess the relevance of Pparα as a molecular mediator of the hypoxia tolerance, we knocked down Pparα in hindlimb muscles of Phd1-deficient mice by electroporating constructs encoding selective interference RNAs against Pparα ($shPpar\alpha^{KD}$). Knockdown of Pparα completely abolished the hypoxia tolerance of Phd1-deficient myofibers (**Fig. 5a**,**b**). Notably, pretreatment of wild-type mice with the Pparα agonist fenofibrate caused the opposite effect and induced hypoxia tolerance (necrotic muscle area: 5.7 ± 0.5 mm^2 in control versus 1.9 ± 0.3 mm^2 after fenofibrate; $n = 4$; $P < 0.001$). Moreover, fenofibrate upregulated the expression of *Ppara* and *Pdk4* (mRNA expression, as a percentage of wild-type expression: 177 ± 4% for *Ppara*; $n = 7$; $P = 0.01$; 245 ± 5% for *Pdk4*; $n = 7$; $P = 0.01$).

Phd1$^{-/-}$ fiber protection is regulated mainly via Hif-2α

Loss of Hif-2α results in mitochondrial dysfunction and skeletal myopathy[30]. We therefore speculated that Hif-2α might be a downstream target of Phd1 conferring muscle resistance to ischemia. Indeed, immunoblotting showed elevated Hif-2α concentrations in

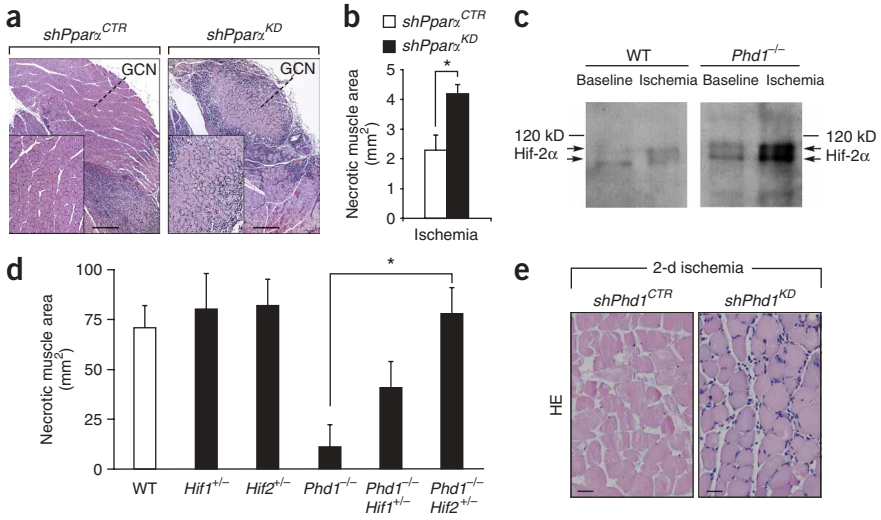

Figure 5 Role of Pparα and Hif-2α, and hypoxia tolerance by knockdown of Phd1. (**a**) Hematoxylin-eosin staining of Phd1-deficient muscles (48 h of ischemia) after shRNA-mediated knockdown of Pparα, or electroporation with a *shPparα*^{CTR} construct, showing hypoxia tolerance in control Phd1-deficient muscle and reversal of this phenotype upon knockdown of Pparα. Inset shows gastrocnemius (GCN) muscle at higher magnification. (**b**) Muscle necrosis at 2 d of ischemia indicating lack of ischemic muscle protection in Phd1-deficient mice after knockdown of Pparα. * $P < 0.005$ versus control; $n = 6$. (**c**) Immunoblot showing higher Hif-2α protein concentrations in Phd1-deficient versus wild-type muscle (6 h of ischemia). In baseline conditions, Hif-2α levels were at the limit of detection but, when detectable (as shown in this panel), Hif-2α concentrations were also higher in Phd1-deficient muscle. Equal amounts of protein were loaded. (**d**) Analysis of muscle necrosis at 7 d of ischemia showing that myofibers were protected against ischemic necrosis in Phd1-deficient (*Egln2*$^{-/-}$) mice and *Egln2*$^{-/-}$;*Hif1a*$^{+/-}$ mice, but not in *Egln2*$^{-/-}$;*Epas1*$^{+/-}$ mice. * $P = 0.001$ by univariate analysis with Bonferroni correction for multiple testing and after Mann-Whitney ($n = 6$). (**e**) Hematoxylin-eosin staining of heterozygous Phd1-deficient (*Egln2*$^{+/-}$) limb muscles (at 48 h after ischemia) after shRNA-mediated knockdown of Phd1 or electroporation with a mismatched shRNA-control construct reveals protection against muscle necrosis upon knockdown of Phd1, but not in control-injected wild-type muscle. Scale bars: 10 μm in **a**,**b**; 25 μm in **e**. WT, wild type.

Phd1-deficient skeletal muscle in ischemia (**Fig. 5c**). In baseline conditions, Hif-2α concentrations were variably detectable, but, when measurable, they were higher in Phd1-deficient muscle (**Fig. 5c**). By contrast, Hif-1α protein expression was low or undetectable in both genotypes in baseline and ischemic conditions (data not shown). Moreover, baseline *Epas1* (encoding Hif-2α) expression was fivefold more abundant than *Hif1a* (encoding Hif-1α) in muscle of both genotypes (mRNA copies per 10^4 copies of β-actin (*Actb* mRNA): 41 ± 2.6 for *Epas1* versus 8.2 ± 0.3 for *Hif1a*; $n = 6$).

To further assess whether ischemic muscle protection in Phd1-deficient mice was dependent on Hif-2α, we intercrossed Phd1-deficient mice with animals lacking one copy of *Epas1* (as loss of both *Epas1* alleles caused embryonic death[31]). Heterozygous loss of *Epas1* completely abrogated the hypoxia tolerance in Phd1-deficient (*Egln2*$^{-/-}$) mice (necrotic muscle area: 7.3 ± 1.0 mm^2 in wild-type mice versus 1.7 ± 1.1 mm^2 in *Egln2*$^{-/-}$ mice and 7.7 ± 1.1 mm^2 in *Egln2*$^{-/-}$;*Epas1*$^{+/-}$ mice; $n = 10$; $P < 0.001$ for *Egln2*$^{-/-}$;*Epas1*$^{+/-}$ versus *Egln2*$^{-/-}$ mice by univariate analysis with Bonferroni correction for multiple testing and by Mann-Whitney test; **Fig. 5d**). In contrast, heterozygous loss of *Hif1a* caused intermediate protection; however, this effect did not reach statistical significance (necrotic muscle area: 3.5 ± 1.1 mm^2 in *Egln2*$^{-/-}$;*Hif1a*$^{+/-}$ mice; $n = 8$; $P = 0.24$ versus *Egln2*$^{-/-}$ mice; **Fig. 5d**).

Phd1 knockdown induces hypoxia tolerance in *Egln2*$^{+/-}$ mice

Our genetic data indicate that germline inactivation of Phd1 protects skeletal muscle against ischemic necrosis. To assess the putative therapeutic relevance of this finding, we tested whether short-term inhibition of Phd1 in adult wild-type mice would provide similar protection. Because selective PHD inhibitors were not available, we used DNA constructs designed to produce short hairpin interference RNA to knock down Phd1 expression: *shPhd1*^{KD} and a control *shPhd1*^{CTR}, which differed by a mismatch of ten nucleotides. The efficiency and specificity of *shPhd1*^{KD} and *shPhd1*^{CTR} were tested *in vitro* (**Supplementary Note**). Electroporation of *shPhd1*^{KD} into *Egln2*$^{+/-}$ muscle reduced *Egln2* (encoding Phd1) transcripts to 23 ± 4% ($n = 13$; $P < 0.001$) of the levels normally detected in wild-type muscle, whereas a similar dose of *shPhd1*^{CTR} was ineffective (83 ± 5% of non-electroporated *Egln2*$^{+/-}$ muscle; $n = 13$; $P = 0.2$).

Histological analysis 2 d after femoral artery ligation showed that *shPhd1*^{CTR} insignificantly reduced necrosis of *Egln2*$^{+/-}$ muscle (necrotic area: 5.5 ± 1.2 × 10^{-1} mm^2 in non-electroporated versus 3.7 ± 1.1× 10^{-1} mm^2 after *shPhd1*^{CTR}; $n = 13$; P = n.s.). By contrast, electroporation of *shPhd1*^{KD} reduced necrosis of *Egln2*$^{+/-}$ myofibers by 83% and 74% compared to non-electroporated or *shPhd1*^{CTR}-injected muscle, respectively (necrotic area: 0.9 ± 0.3 × 10^{-1} mm^2 after *shPhd1*^{KD}; $n = 13$; $P < 0.005$ versus non-electroporated and $P < 0.05$ versus *shPhd1*^{CTR} by *t*-test and Mann-Whitney test; **Fig. 5e**). Thus, similar to germline Phd1 inactivation, knockdown of Phd1 rendered myofibers hypoxia tolerant.

DISCUSSION

Over millions of years of evolution, organisms have developed mechanisms to exploit the metabolic energy potential of oxygen. However, oxygen is not always sufficiently available to allow oxidative metabolism. Moreover, oxygen is also a source of reactive oxygen species that, in excess, may be toxic and harmful. Mechanisms are thus necessary to control the switch from aerobic to anaerobic metabolism and to regulate oxygen consumption. Our genetic study shows that Phd1, which acts as an oxygen sensor, controls this switch in skeletal muscle *in vivo* and, in doing so, determines hypoxia tolerance. The metabolic alterations underlying the hypoxia tolerance are schematically depicted in **Figure 6**.

A molecular mechanism linking oxygen sensing and consumption has not been firmly established. Although HIF-1α regulates oxygen consumption through PDK1 *in vitro*[3,4], it was hitherto unknown whether such regulation was relevant *in vivo*, whether it relied on a reduction in glucose acid oxidation, and, if so, whether it was

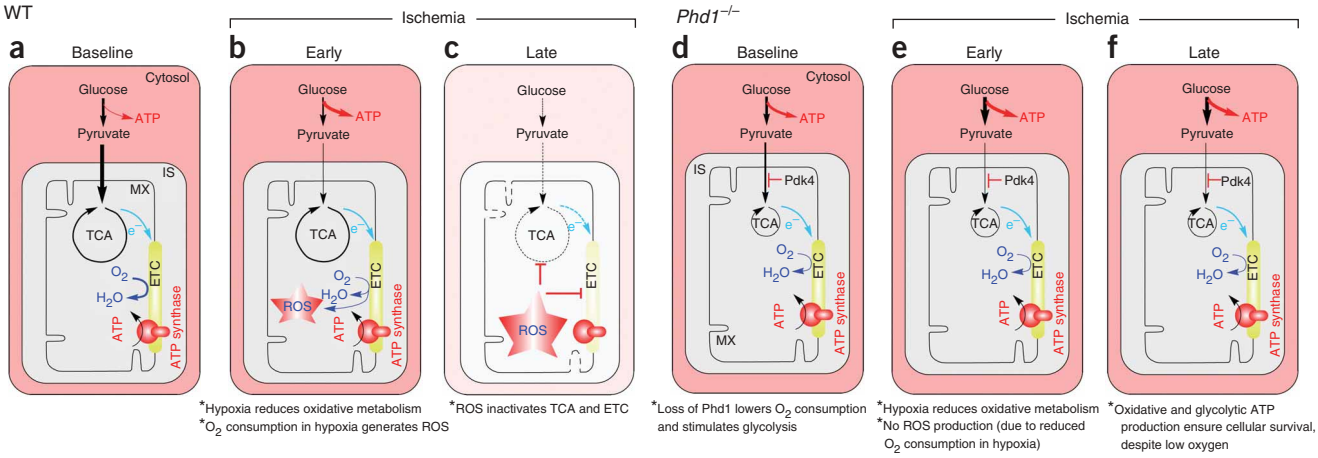

Figure 6 Loss of Phd1 induces hypoxia tolerance. (**a**) Baseline energy metabolism in wild-type myofibers: ATP is generated by anaerobic glycolysis (cytosol) and by glucose oxidation in the TCA cycle (mitochondrial matrix; MX), where it provides electrons (e^-) for the mitochondrial electron-transport chain (ETC; yellow) that consequently drives the synthesis of ATP by the ATP synthase (red). (**b**,**c**) Lethal response to hypoxia in ischemic wild-type myofibers. As a result of the reduced oxygen supply, oxidative phosphorylation is reduced. Nonetheless, ischemic wild-type myofibers continue to consume oxygen, thereby generating excess ROS within the ETC (**b**). This increase in oxidative stress inactivates TCA and ETC enzymes (red line) during prolonged ischemia (**c**), ultimately causing irreversible mitochondrial damage (cristolysis, indicated by dotted line) and complete shutdown of oxidative energy metabolism. Anaerobic glycolysis cannot compensate for the loss of oxidative ATP production, leading to cellular energy exhaustion and demise. (**d**) Baseline metabolic reprogramming in Phd1-deficient myofibers. Enhanced expression of Pdk4 reduces glucose oxidation and oxygen consumption in Phd1-deficient myofibers. Coincidently, loss of Phd1 stimulates glycolytic production of ATP. (**e**,**f**) Hypoxia tolerance in Phd1-deficient myofibers. Reduced oxygen consumption leads to attenuated ROS formation in ischemic Phd1-deficient myofibers (**e**). As a consequence, enzymes in the TCA and ETC are not (or are less) inactivated (**f**), thereby enabling residual oxidative phosphorylation (albeit lower than in baseline conditions because of the reduced oxygen supply). In addition, increased glycolysis together with the residual respiration provides sufficient ATP for survival. WT, wild type.

accompanied by a change in fatty acid oxidation. Our studies show that, in the absence of Phd1, oxygen consumption is reduced in skeletal muscle *in vivo*, and that oxygen conservation is attributable to a selective decrease in glucose oxidation, without alterations in fat combustion. At the molecular level, loss of Phd1 upregulates Pdk1 and Pdk4; both PDKs restrict the entry of glycolytic intermediates into the TCA cycle by inhibiting the activity of PDC[32]. However, a consequence of this is that oxidative muscle performance is impaired in healthy Phd1-deficient mice.

Loss of Phd1 induces hypoxia tolerance in myofibers to a sufficient extent that these cells are protected against acute severe hypoxia, which is lethal for wild-type cells. The rapidity of this protection implies a reprogramming of basal metabolism that 'prepares' Phd1-deficient mice to cope better with such acute ischemic insults. Indeed, by decreasing glucose oxidation, oxygen consumption is reduced in Phd1-deficient myofibers in baseline conditions; precisely because of this conservation of oxygen, Phd1-deficient myofibers generate less oxidative stress in ischemic conditions (see below). As a result, mitochondrial structure and performance are not irreversibly damaged, allowing ischemic Phd1-deficient mitochondria to maintain a critical residual degree of oxidative phosphorylation. Thus, almost paradoxically, the reduced respiration in baseline conditions is the very mechanism that ultimately ensures continuing respiration in ischemic conditions in Phd1-deficient myofibers. Because Phd1 has a substantially higher K_m for oxygen than cytochrome *c* oxidase, our findings raise the possibility that Phd1 provides an advance warning function enabling compensatory responses before life-threatening metabolic insufficiency or hypoxia. Of note, the survival benefit in ischemia induced by inactivation of Phd1 comes at the expense of an impaired oxidative muscle performance in healthy conditions.

When oxygen supply is limiting, mitochondrial respiration declines, and cells shift to anaerobic energy production. The EPR measurements indicate that oxygen supply was reduced in ischemia by ~80% in both wild-type and Phd1-deficient mice. Hence, respiration was expected to be comparably reduced in both genotypes. However, when hypoxia is severe and sustained (as in our model), mitochondrial performance is further suppressed by oxidative damage[33,34]. ROS are a normal by-product of the electron transfer chain in aerobic conditions, but, when mitochondria keep consuming oxygen in hypoxic conditions, ROS are generated in excess (**Fig. 6b**)[3,4]. The pimonidazole results indicate that ischemic wild-type myofibers continued to consume oxygen despite the limited oxygen supply. Several lines of evidence indicate that ischemic wild-type myofibers then generated excessive amounts of ROS and that mitochondrial respiration progressively declined until it was completely eliminated. At this stage, ischemic wild-type myofibers could no longer generate ATP and died (**Fig. 6c**). In contrast, because of the metabolic adaptation, ischemic Phd1-deficient myofibers consumed less oxygen and thereby generated less oxidative stress. As a result, respiration was not entirely eliminated, and mitochondria remained capable of oxidative phosphorylation, albeit at a much reduced level compared to that in normoxic conditions (**Fig. 6e**).

Besides the better preservation of oxidative phosphorylation, enhanced glycolysis further protects ischemic Phd1-deficient myofibers against metabolic demise. Concomitant with the decrease in glucose oxidation (by ~30%), glycolysis was comparably increased (by ~30%) in Phd1-deficient muscle in baseline conditions. We did not detect major changes in glycolytic enzyme concentrations in Phd1-deficient muscle, perhaps because Hif-2α is a more important mediator than Hif-1α in these mice. However, mitochondrial respiration and glycolytic flux are known to be tightly coupled to ensure ATP production under conditions of varying oxygen supply (Pasteur effect)[35]. Indeed, cells strive to maintain the cellular energy charge ([ATP] + 0.5[ADP] / [ATP] + [ADP] + [AMP]) within narrow limits

between 0.8 and 0.95. Thus, in aerobic conditions, glucose is oxidatively metabolized, yielding energy at high efficiency (about 30 moles ATP per mole glucose). In contrast, in anaerobic conditions, glucose is glycolytically metabolized by glycolysis, with reduced energy production (2 moles ATP per mole glucose). Because ATP is an allosteric inhibitor of phosphofructokinase, a decrease in energy charge will accelerate glycolytic flux to restore ATP levels. Hence, the increase in anaerobic metabolism may be secondary to the decrease in mitochondrial respiration in Phd1-deficient mice, though other mechanisms cannot be excluded.

The upregulation of *Epas1* (encoding Hif-2α) in Phd1-deficient muscle, the more abundant expression of *Epas1* than *Hif1a* in muscle, and the reversal of hypoxia tolerance in *Egln2*$^{-/-}$;*Epas1*$^{+/-}$ mice all indicate that Hif-2α is, at least in part, a downstream mediator of Phd1 in hypoxia tolerance. Moreover, heterozygous loss of *Epas1* partially normalized the elevated expression of *Pdk4* and *Ppara* (data not shown). A role for Hif-2α in the hypoxia tolerance pathway is also consistent with findings that loss of Hif-2α causes generalized oxidative stress[30]. HIF-1α also seems to be involved in the PHD1 pathway, although perhaps less prominently, likely by regulating the expression of PDK1 (refs. 3,4). Of note, others previously documented a role of HIF-1α in skeletal muscle metabolism[16].

An intriguing observation is that Pparα seems to act downstream of Phd1. Pparα is expressed in oxidative muscle fibers and is a transcriptional master regulator of metabolism[18,36]. The coincident upregulation of *Ppara* and *Pdk4* in Phd1-deficient mice is consistent with the known mode of action of this regulator to reduce glucose oxidation through induction of Pdk4. Moreover, the phenocopying of the hypoxia tolerance in Phd1-deficient mice by the fenofibrate-induced activation of Pparα in wild-type mice, together with the loss of hypoxia tolerance of Phd1-deficient mice by knockdown of Pparα, strongly suggest that Pparα is a downstream mediator of the observed hypoxia tolerance. As no HIF-binding site is readily detectable in the *Pdk4* gene regulatory sequences, Phd1 may control the expression of *Pdk4* through Pparα. Our data do not exclude a possible involvement of other metabolic regulators downstream of Phd1. Because loss of Phd1 did not affect fatty acid oxidation (which is stimulated by Pparα), we speculate that the elevated concentrations of Pparα were sufficient to affect glucose oxidation, but insufficient to alter fat combustion. Another outstanding molecular question is whether and how Hif-2α regulates the expression of Pparα.

Our genetic study yielded additional intriguing findings. First, loss of Phd1 (*Egln2*$^{-/-}$), but not of Phd2 (*Egln1*$^{+/-}$) or Phd3 (*Egln3*$^{-/-}$), selectively induced hypoxia tolerance, indicating that, even though all PHDs are expressed in myofibers, they are likely to have specific physiological roles. Our data do not exclude the possibility that Phd2 loss of function may provide muscle protection, as we did not delete both *Egln1* alleles. Second, hypoxia tolerance was not due to enhanced angiogenesis, vasodilation or erythropoiesis, even though each of them is presumably regulated by PHD activity. Third, few genetic mouse models of hypoxia tolerance exist[21,37]. Notably, Phd1-deficient mice show features that also occur in hypoxia-tolerant humans and animals. For instance, similarly to Phd1-deficient mice, hibernating species show upregulated PDK4 and PPARα[38]. Hence, the Phd1-deficient mouse may constitute a new tool to unravel the enigmatic molecular basis of hibernation and other conditions of hypoxia tolerance.

Germline inactivation of Phd1 reprogrammed metabolism, and this was associated with improved outcome from an acute episode of severe tissue hypoxia. Of note, this metabolic reprogramming did not require germline manipulation, as Phd1 knockdown resulted in similar effects in adult mice. The rapidity with which PCr levels started to recover (within 30 min after femoral artery ligation) indicates that this metabolic reprogramming allowed Phd1-deficient mice to react almost instantaneously. One implication of this is that physiological regulation of Phd1 activity could provide rapid, reversible metabolic adaptation when animals enter hibernation and become hypoxia tolerant[1]. Hypoxia tolerance also promotes cancer malignancy[39,40], and oxidative stress has been implicated in health, longevity and numerous diseases[41,42]. In other cases, induction of hypoxia tolerance might be of therapeutic value to improve organ preservation for transplantation. The insight that Phd1 controls hypoxia tolerance and the response to oxidative stress warrants further analysis of its possible involvement in these processes. Notably, our findings also suggest that pharmacological inhibition of PHD1 may provide a useful means to protect muscle, and potentially other organs, from ischemic injury.

METHODS

Quantitative real-time RT-PCR and protein blotting. mRNA transcript expression was quantified by real-time RT-PCR and normalized relative to the expression of *Actb* or *Gapdh* using gene-specific primers and probes labeled with fluorescent dye (FAM) and quencher (TAMRA; for a detailed list of primers and probes, see **Supplementary Table 1** online). We prepared whole tissue lysates in either lysis buffer (Tris base 10 mM pH 6.8 room temperature, 8 M urea, 1% SDS buffer) or RIPA buffer. Nuclear extracts were prepared with a commercial kit (Pierce). For protein blotting, 100 μg of protein was fractionated by SDS-PAGE and transferred onto nitrocellulose membranes (Hybond-ECL). We incubated membranes with specific antibodies against Phd1 (ref. 8), Phd2 and Phd3 (Bethyl Laboratories), desmin (Abcam), Pdk1 (Assay designs, Inc.), Pdk4 (custom produced by Sigma-Genosys) and Vdac1 (Santa Cruz). Bound primary antibody was visualized with a species-specific horseradish peroxidase–conjugated secondary antibody (DakoCytomation) and chemiluminescence system (Pierce).

Histology, immunostaining, morphometry and ischemia mouse model. Crural muscles were dissected, fixed in 4% PFA, dehydrated, embedded in paraffin and sectioned at 10-μm thickness. After deparaffinization and rehydration, sections were digested with 0.2% trypsin (Sigma), blocked and incubated overnight with primary antibodies. We used the following as primary antibodies: rabbit anti-PHD1 (ref. 8), rat anti-Cd31 (BD Pharmingen; dilution 1/500), rat anti–caspase-3 (Gentaur-Biovision; dilution 1/20) and mouse anti-8OHdG (Oxis International; dilution 1/20). Sections were subsequently incubated with appropriate secondary antibodies, developed with 3,3′-diaminobenzidine (DAB, Sigma) and counterstained with Harris hematoxylin. For detection of hypoxic cells, we treated mice with pimonidazole (Chemicon) for 1 h before dissection of muscles; we then stained muscle sections with the Hydroxyprobe-1 antibody (Chemicon) according to the manufacturer's instructions. Metabolic fiber properties were assessed on consecutive cryostat sections (12 μm) of snap frozen crural muscles, which were subjected to histochemical mATPase staining (pH 4.1) according to standard protocols. Limb ischemia was done as described elsewhere[43].

EPR oximetry *in vivo*. We measured muscle pO_2 using charcoal powder (100 μg; CX0670-1; EM Science) as the oxygen-sensitive probe. Calibration curves were made by measuring the EPR line width as a function of the pO_2 (ref. 44). We implanted charcoal bilaterally into the gastrocnemius muscles of Phd1-deficient and wild-type mice 1 week before unilateral right ligation of the femoral vessels, and recorded EPR spectra of both legs at 2, 4, 6 and 24 h after vascular ligation using an EPR spectrometer (Magnetech) with a low-frequency microwave bridge operating at 1.1 GHz and extended loop resonator.

Protein carbonylation. The presence of carbonyl groups in proteins was determined in gastrocnemius supernatant fractions using a commercial kit (Oxyblot, Chemicon International) according to the manufacturer's instructions. Carbonyl groups were derivatized to 2,4-dinitro-phenylhydrazone (DNP-hydrazone) by reaction with 2,4-dinitro-phenylhydrazine (DNPH),

and DNP-derivatized proteins were detected by protein blotting using a specific antibody against the DNP moiety of the proteins.

Indirect calorimetry assay. Oxygen consumption was simultaneously determined on *ad libitum* fed, group-housed animals (group A: $n = 5$ for each genotype, group B: $n = 7$ for each genotype, 12-week-old, male and female mice) through indirect calorimetry by using an open-circuit calorimeter unit[45].

Mitochondrial respiration in permeabilized myofibers. We determined mitochondrial respiration in small bundles of saponin-permeabilized myofibers from wild-type and Phd1-deficient soleus muscle using high-resolution respirometry (Oroboros Oxygraph-2k), using the DatLab Software for data acquisition and analyses (Oroboros Instruments), as previously described[46–48].

NMR spectroscopy. We carried out *in vivo* ^{31}P-NMR spectroscopy experiments on lower limbs at 188 MHz in a Bruker Biospec, equipped with a horizontal 4.7 T superconducting magnet, using a 10-mm diameter solenoid transmit-receive coil. *In vivo* determination of glucose and fatty acid oxidation rates in the hindlimbs was performed using [U-^{13}C]glucose and [U-^{13}C]fatty acids, respectively.

Running test. We tested forced exercise endurance in a treadmill graded exercise test with an initial velocity of 6 m/min and an increase in velocity of 2 m/min every 5 min. Mice were running at a 10° incline (uphill) to induce concentric exercise in the crural musculature, which recruits primarily oxidative muscle fibers.

Glycolysis in isolated soleus. We dissected soleus muscles and incubated them for 4 h at 37 °C in KHB buffer (116 mM NaCl, 5.4 mM KCl, 1.8 mM $CaCl_2$, 0.4 mM $MgSO_4$, 0.91 mM KH_2PO_4, 26.2 mM $NaHCO_3$, pH 7.4) containing 5 mM glucose/80 μCi/mmol [5-^{3}H]glucose. The reaction was terminated by addition of perchloric acid, and the muscles were then removed. We captured ^3H_2O in a plastic hanging well containing a H_2O-soaked filter paper for 3 d at 37 °C and determined radioactivity by liquid scintillation counting. The rate of glycolysis was calculated from the difference between the rate of ^3H_2O formation and the rate of substrate recycling. Rate of ^3H_2O capturing was determined using known amounts of ^3H_2O as a standard.

Knockdown of Pparα and Phd1 in mice. *shPparα*^{KD}, *shPhd1*^{KD}, *shPparα*^{CTR} or *shPhd1*^{CTR} pENTR^{TM}/U6 plasmids (40 μg in 30 μl saline) were delivered to the skeletal muscle of Phd1-deficient mice through *in vivo* electroporation[49]. Injected muscles were immediately electroporated with a strain of eight pulses (80 V; duration 0.20 ms; 8 pulses, intervals 1 per sec) using an electroporation system (BTX ECM 830 electroporator; Genetronix) with Tweezertrode circular electrodes (7-mm diameter). Electroporation was carried out 5 d before induction of limb ischemia and was followed by the analysis of muscle necrosis.

Statistical methods. The data were represented as mean ± s.e.m. of the indicated number of measurements. Standard *t*-tests were used to calculate significance levels between groups. ANOVA univariate analysis was used to correct *P* values for multiple comparisons against a single wild-type group (Dunnett's correction for multiple testing) or against various groups (Bonferroni correction for multiple testing). In the hindlimb ischemia model, muscle necrosis was absent in some of the germline Phd1-deficient or Phd1-knockdown mice (indicative of complete protection against muscle damage), thereby disturbing normal Gaussian distribution as calculated by Shapiro-Wilk tests. In these cases, we used nonparametrical Mann-Whitney tests to calculate statistical significance between these groups. The *P* values obtained by ANOVA remained significant when correcting for the total muscle area analyzed. We used SPSS (version 11.0 for Mac OS X) for all these calculations.

Note: Supplementary information is available on the Nature Genetics website.

ACKNOWLEDGMENTS

J.A. is sponsored by the Centro Nacional de Investigaciones Cardiovasculares (CNIC; Spain) and Flanders Institute of Biotechnology (VIB; Belgium); M.S. by the Deutsche Forschungsgemeinschaft (Germany) and the Lymphatic Research Foundation; K.V.G. by a doctoral fellowship from the K.U. Leuven; P.F. by a postdoctoral fellowship from the K.U. Leuven; and H.L. by a postdoctoral fellowship from Fond Québécois de la nature et des technologies. This work is supported, in part, by grant GOA2006/11/KULeuven from the University of Leuven, Belgium, grant IUAP05/02 from the Federal Government Belgium, grants FWO G.0265 and FWO G.0387 from the Flanders Research Foundation, Belgium, grant 5RO1GM037704 from the US National Institutes of Health (to F.L.), grant 12RO1DK47844 from the US National Institutes of Health (to R.A.H.), grant 2.4532.03 from the Belgian Fonds National de la Recherche Scientifique (to F.S.), and a grant from the Molecular Small Animal Imaging Center, University of Leuven (to L.M. and P.V.H.) and by a Programme Grant from the British Heart Foundation (to P.H.M. and P.J.R.). The authors thank A. Bouche, A. Carton, P. Chevron, M. De Mol, E. Gils, B. Hermans, L. Kieckens, W.Y. Man, W. Martens, A. Manderveld, E. Meyhi, L. Notebaert, J. Souffreau, C. Vanhuylebroeck, B. Vanwetswinkel, P. Van Wesemael, Q. Swennen, B. Kamers and S. Wyns for their contributions.

AUTHOR CONTRIBUTIONS

J.A.: analysis of all data; design and performance of NMR spectroscopy, assays of metabolic enzymes, metabolites, indirect calorimetry, RNA and protein expression, and respiration studies; writing of the paper. M.S.: analysis of all data; design and performance of running tests, hind limb vascularization, EPR, respiration studies, indirect calorimetry and histological analysis; writing of the paper. K.V.G.: analysis of all data; design and performance of RNA interference experiments, metabolic assays, indirect calorimetry and RNA and protein expression; writing of the paper. P.F.: analysis of all data; design and performance of metabolic assays and mitochondrial respiration studies; writing of the paper. T.D. and P.V.H.: NMR spectroscopy. M.M., P.L., S.K.H., A.G., S.Z. and T.B.: protein expression analysis, cell culture experiments, mitochondrial performance assays. N.H.J., F.G., R.A.H. and R.D.: metabolic enzyme and metabolite assays; oxidative stress assays. D.L. and M.D.: generation of PHD1-deficient mice; genetic analysis of background; statistical analysis. A.D.-J. and T.V.: design of constructs expressing interference short hairpin RNAs. P.V.N., K.D.B. and P.H.: muscle exercise studies. C.W. and C.P.: design and construction of PHD1 targeting vector. M.T. and L. Moons.: histological analysis. R.N. and F. Sluse.: mitochondrial respiration studies. C.D., B.W., J.N. and L. Mortelmans: glucose metabolism studies. B.J. and B.G.: EPR studies. R.S.-M. and F.L.: mitochondrial ultrastructure. P.S.: micro-CT analysis. J.B.: indirect calorimetry. H.L. and E.G.: analysis and performance of mitochondrial respiration studies in isolated myofibers. P.V.V., F. Schuit and M.B.: analysis and design of metabolic experiments and oxidative stress assays; writing of the paper. P.R., P.M and P.C.: scientific direction; generation of PHD knockout mice; conception of hypoxia tolerance studies; design of experimental approaches; analysis of data; writing of the paper.

COMPETING INTERESTS STATEMENT

The authors declare competing financial interests: details accompany the full-text HTML version of the paper at http://www.nature.com/naturegenetics/.

Published online at http://www.nature.com/naturegenetics
Reprints and permissions information is available online at http://npg.nature.com/reprintsandpermissions

1. Ramirez, J.M., Folkow, L.P. & Blix, A.S. Hypoxia tolerance in mammals and birds: from the wilderness to the clinic. *Annu. Rev. Physiol.* **69**, 113–143 (2007).
2. Andrews, M.T. Genes controlling the metabolic switch in hibernating mammals. *Biochem. Soc. Trans.* **32**, 1021–1024 (2004).
3. Kim, J.W., Tchernyshyov, I., Semenza, G.L. & Dang, C.V. HIF-1-mediated expression of pyruvate dehydrogenase kinase: a metabolic switch required for cellular adaptation to hypoxia. *Cell Metab.* **3**, 177–185 (2006).
4. Papandreou, I., Cairns, R.A., Fontana, L., Lim, A.L. & Denko, N.C. HIF-1 mediates adaptation to hypoxia by actively downregulating mitochondrial oxygen consumption. *Cell Metab.* **3**, 187–197 (2006).
5. Sugden, M.C. & Holness, M.J. Mechanisms underlying regulation of the expression and activities of the mammalian pyruvate dehydrogenase kinases. *Arch. Physiol. Biochem.* **112**, 139–149 (2006).
6. Bruick, R.K. & McKnight, S.L. A conserved family of prolyl-4-hydroxylases that modify HIF. *Science* **294**, 1337–1340 (2001).
7. Epstein, A.C. *et al. C. elegans* EGL-9 and mammalian homologs define a family of dioxygenases that regulate HIF by prolyl hydroxylation. *Cell* **107**, 43–54 (2001).
8. Appelhoff, R.J. *et al.* Differential function of the prolyl hydroxylases PHD1, PHD2, and PHD3 in the regulation of hypoxia-inducible factor. *J. Biol. Chem.* **279**, 38458–38465 (2004).
9. Berra, E. *et al.* HIF prolyl-hydroxylase 2 is the key oxygen sensor setting low steady-state levels of HIF-1alpha in normoxia. *EMBO J.* **22**, 4082–4090 (2003).
10. Elson, D.A. *et al.* Induction of hypervascularity without leakage or inflammation in transgenic mice overexpressing hypoxia-inducible factor-1α. *Genes Dev.* **15**, 2520–2532 (2001).

11. Willam, C. *et al.* Peptide blockade of HIFα degradation modulates cellular meta bolism and angiogenesis. *Proc. Natl. Acad. Sci. USA* **99**, 10423–10428 (2002).
12. Takeda, K. *et al.* Placental but not heart defects are associated with elevated hypoxia-inducible factor α levels in mice lacking prolyl hydroxylase domain protein 2. *Mol. Cell. Biol.* **26**, 8336–8346 (2006).
13. Hochachka, P.W. Mechanism and evolution of hypoxia-tolerance in humans. *J. Exp. Biol.* **201**, 1243–1254 (1998).
14. Schuler, M. *et al.* PGC1α expression is controlled in skeletal muscles by PPARβ, whose ablation results in fiber-type switching, obesity, and type 2 diabetes. *Cell Metab.* **4**, 407–414 (2006).
15. Kotani, K., Peroni, O.D., Minokoshi, Y., Boss, O. & Kahn, B.B. GLUT4 glucose transporter deficiency increases hepatic lipid production and peripheral lipid utilization. *J. Clin. Invest.* **114**, 1666–1675 (2004).
16. Mason, S.D. *et al.* Loss of skeletal muscle HIF-1α results in altered exercise endurance. *PLoS Biol.* **2**, e288 (2004).
17. Sloniger, M.A., Cureton, K.J., Prior, B.M. & Evans, E.M. Lower extremity muscle activation during horizontal and uphill running. *J. Appl. Physiol.* **83**, 2073–2079 (1997).
18. Finck, B.N. *et al.* A potential link between muscle peroxisome proliferator-activated receptor-α signaling and obesity-related diabetes. *Cell Metab.* **1**, 133–144 (2005).
19. Jeoung, N.H. *et al.* Role of pyruvate dehydrogenase kinase isoenzyme 4 (PDHK4) in glucose homeostasis during starvation. *Biochem. J.* **397**, 417–425 (2006).
20. Harris, R.A., Bowker-Kinley, M.M., Huang, B. & Wu, P. Regulation of the activity of the pyruvate dehydrogenase complex. *Adv. Enzyme Regul.* **42**, 249–259 (2002).
21. Zaccagnini, G. *et al.* p66ShcA modulates tissue response to hindlimb ischemia. *Circulation* **109**, 2917–2923 (2004).
22. Bracken, C.P., Whitelaw, M.L. & Peet, D.J. The hypoxia-inducible factors: key transcriptional regulators of hypoxic responses. *Cell. Mol. Life Sci.* **60**, 1376–1393 (2003).
23. Doege, K., Heine, S., Jensen, I., Jelkmann, W. & Metzen, E. Inhibition of mitochondrial respiration elevates oxygen concentration but leaves regulation of hypoxia-inducible factor (HIF) intact. *Blood* **106**, 2311–2317 (2005).
24. Clanton, T.L. Hypoxia-induced reactive oxygen species formation in skeletal muscle. *J. Appl. Physiol.* **102**, 2379–2388 (2007).
25. Fiskum, G. *et al.* Protection against ischemic brain injury by inhibition of mitochondrial oxidative stress. *J. Bioenerg. Biomembr.* **36**, 347–352 (2004).
26. Imai, H., Graham, D.I., Masayasu, H. & Macrae, I.M. Antioxidant ebselen reduces oxidative damage in focal cerebral ischemia. *Free Radic. Biol. Med.* **34**, 56–63 (2003).
27. Ott, M., Gogvadze, V., Orrenius, S. & Zhivotovsky, B. Mitochondria, oxidative stress and cell death. *Apoptosis* **12**, 913–922 (2007).
28. Gardner, P.R. Aconitase: sensitive target and measure of superoxide. *Methods Enzymol.* **349**, 9–23 (2002).
29. Wu, P., Peters, J.M. & Harris, R.A. Adaptive increase in pyruvate dehydrogenase kinase 4 during starvation is mediated by peroxisome proliferator-activated receptor alpha. *Biochem. Biophys. Res. Commun.* **287**, 391–396 (2001).
30. Scortegagna, M. *et al.* Multiple organ pathology, metabolic abnormalities and impaired homeostasis of reactive oxygen species in *Epas1*$^{-/-}$ mice. *Nat. Genet.* **35**, 331–340 (2003).
31. Brusselmans, K. *et al.* Heterozygous deficiency of hypoxia-inducible factor-2α protects mice against pulmonary hypertension and right ventricular dysfunction during prolonged hypoxia. *J. Clin. Invest.* **111**, 1519–1527 (2003).
32. Sugden, M.C. & Holness, M.J. Recent advances in mechanisms regulating glucose oxidation at the level of the pyruvate dehydrogenase complex by PDKs. *Am. J. Physiol. Endocrinol. Metab.* **284**, E855–E862 (2003).
33. Becker, L.B., vanden Hoek, T.L., Shao, Z.H., Li, C.Q. & Schumacker, P.T. Generation of superoxide in cardiomyocytes during ischemia before reperfusion. *Am. J. Physiol.* **277**, H2240–H2246 (1999).
34. Magalhaes, J. *et al.* Acute and severe hypobaric hypoxia increases oxidative stress and impairs mitochondrial function in mouse skeletal muscle. *J. Appl. Physiol.* **99**, 1247–1253 (2005).
35. Thomas, S. & Fell, D.A. A control analysis exploration of the role of ATP utilisation in glycolytic-flux control and glycolytic-metabolite-concentration regulation. *Eur. J. Biochem.* **258**, 956–967 (1998).
36. Lefebvre, P., Chinetti, G., Fruchart, J.C. & Staels, B. Sorting out the roles of PPARα in energy metabolism and vascular homeostasis. *J. Clin. Invest.* **116**, 571–580 (2006).
37. Haddad, G.G. Tolerance to low O_2: lessons from invertebrate genetic models. *Exp. Physiol.* **91**, 277–282 (2006).
38. Buck, M.J., Squire, T.L. & Andrews, M.T. Coordinate expression of the PDK4 gene: a means of regulating fuel selection in a hibernating mammal. *Physiol. Genomics* **8**, 5–13 (2002).
39. Semenza, G.L. Targeting HIF-1 for cancer therapy. *Nat. Rev. Cancer* **3**, 721–732 (2003).
40. Wouters, B.G., van den Beucken, T., Magagnin, M.G., Lambin, P. & Koumenis, C. Targeting hypoxia tolerance in cancer. *Drug Resist. Updat.* **7**, 25–40 (2004).
41. Balaban, R.S., Nemoto, S. & Finkel, T. Mitochondria, oxidants, and aging. *Cell* **120**, 483–495 (2005).
42. Wallace, D.C. Mitochondrial diseases in man and mouse. *Science* **283**, 1482–1488 (1999).
43. Luttun, A. *et al.* Revascularization of ischemic tissues by PlGF treatment, and inhibition of tumor angiogenesis, arthritis and atherosclerosis by anti-Flt1. *Nat. Med.* **8**, 831–840 (2002).
44. Jordan, B.F. *et al.* Insulin increases the sensitivity of tumors to irradiation: involvement of an increase in tumor oxygenation mediated by a nitric oxide-dependent decrease of the tumor cells oxygen consumption. *Cancer Res.* **62**, 3555–3561 (2002).
45. Buyse, J. *et al.* Energy and protein metabolism between 3 and 6 weeks of age of male broiler chickens selected for growth rate or for improved food efficiency. *Br. Poult. Sci.* **39**, 264–272 (1998).
46. Kuznetsov, A.V. *et al.* Mitochondrial defects and heterogeneous cytochrome c release after cardiac cold ischemia and reperfusion. *Am. J. Physiol. Heart Circ. Physiol.* **286**, H1633–H1641 (2004).
47. Gnaiger, E. Oxygen conformance of cellular respiration. A perspective of mitochondrial physiology. *Adv. Exp. Med. Biol.* **543**, 39–55 (2003).
48. Boushel, R. *et al.* Patients with type 2 diabetes have normal mitochondrial function in skeletal muscle. *Diabetologia* **50**, 790–796 (2007).
49. McMahon, J.M., Signori, E., Wells, K.E., Fazio, V.M. & Wells, D.J. Optimisation of electrotransfer of plasmid into skeletal muscle by pretreatment with hyaluronidase–increased expression with reduced muscle damage. *Gene Ther.* **8**, 1264–1270 (2001).